

INFORMATIONAL ASSOCIATING MODEL BASED ON SPATIAL SCALING OF SATELLITE IMAGES AND APPLICATION

Jianzhong Feng^{a,*}, Huajun Tang^a, Zhongxin Chen^a, S. Qingbo Zhou^a, Linyan Bai^b

^a Key Lab of Resources Remote Sensing & Digital Agriculture, Ministry of Agriculture, Institute of Agricultural Resources and Regional Planning, Chinese Academy of Agricultural Sciences, Beijing, China, 100081

^b National Key Lab of Remote Sensing Science, Institute of Remote Sensing Applications, Chinese Academy of Science, Beijing, China, 100101 - bai_linyan@163.com

Commission VI, WG VI/4

KEY WORDS: Geo-space, Scaling conversion, Multi-resolution, Remote sensing image data, Associating Model

ABSTRACT:

There are a great deal of obvious issues about effects of scale and scaling conversion that need to be solved for agricultural condition monitoring using remote sensing. In this paper, a serial of researches about them were performed so as to service practical requirements of agricultural condition remote sensing monitoring, especially in the dynamic monitoring of crops growth using remote sensing technology, such as suitability of satellite images on different spatial resolution (i.e. spatial scales); associated relationships of some same kind of remote sensing information on different spatial scales in terms of time changes; a set of corresponding spatial-and-temporal associating models developed; and their effectiveness relatively assessed. As for validating the above, a case study was provided in Hengshui region of North China Plain, using multi-temporal satellite imageries of MODIS (Moderate-resolution Imaging Spectroradiometer, spatial resolutions of 500m & 250m) aboard EOS and AVHRR (Advanced Very High Resolution Radiometer, a spatial resolution of 1km) aboard NOAA, wherein the spectral characteristic values such as NDVI (Normalized difference vegetation index) were retrieved and applied in the corresponding spatial resolutions (spatial scales) of the satellite images. Practically, the last results showed that the model and approach of remote sensing scale and scaling conversion were effective and available in the actual crop growing remote sensing monitoring, while preserving informational integrity of satellite imageries, and hence they are able to be more widely applied and further integrated into agricultural condition remote sensing monitoring systems.

1. INTRODUCTION

Scale problems in the field of satellite remote sensing and GIS aroused very early researchers' great concern and attention (Markham et al, 1981; Woodcock et al, 1987; Atkinson et al, 1995; Liu et al, 2004). It is characterised that satellite remote sensing data in different temporal and spatial resolutions (i.e., at temporal and spatial scales) recorded the Earth surface (ES) characteristics, so the environmental monitoring needs remote sensing data in multi-resolution and their relevant applications at associated appropriate scales (i.e. a problem as to adaptive choice of scale), and transfer of the remote sensing information across different scales (Bo et al, 2003). Moreover, scale effect of remote sensing informational model is greatly significant, and there are thus many researches carried on it in order to explore the effective and adaptable scale range of some model application and the synergic relationship between different models at different scales (Liu et al, 2004).

Here, Scale problem is very evident in agricultural condition monitoring using remote sensing, especially being an important limiting factor of effectively monitoring staple crop growth (e.g. in wide areas). For examples, in a sampling solution of remote sensing monitoring, it often results in a greater error that a sampling design (e.g. a size of sample box) does not match the resolution of remote sensing data; the available information is extracted from satellite remote sensing data in different spatial resolutions (at different spatial scales) and during crucial

periods of crops growth, whereas each of their precisions is very different because, too small or too large spatial scale, will affect effect of monitoring crops growth and accuracy of crops yield forecasting and area estimation, which is obviously featured with effect phenomenon of temporal and spatial multi-scale, adaptability of scale of remote sensing monitoring indices and its uncertainty (Wu et al, 2004; Mo et al, 2007).

Given that the operation and running is usually based on large-scale areas (e.g., in national or a few provincial areas), high timeliness and batch data processing in agricultural condition remote sensing monitoring, those tasks thus have to be completed during some limited time period (e.g. in three months term), and then the integrated monitoring is mainly characteristic using multi-source remote sensing data (Qian et al, 2004).

According to the basic theories and methods of remote sensing scaling conversion, this study explored the following contents so as to service practical requirements of agricultural condition remote sensing monitoring, especially in the dynamic monitoring of crops growth, as was shown later: (1) suitability of satellite images in different spatial resolutions (i.e. at spatial scales) is expounded; (2) based on a pyramid architecture of spatial scales, associated relationships of some same kind of remote sensing information at spatial scales were investigated in terms of time changes (i.e. at some selected temporal scales),

* Corresponding author; e-mail: fengjzh4680@sina.com.cn.

and then a set of corresponding spatial-and-temporal associating models were developed; (3) hence, the results of crop growing monitoring using remote sensing technology were emended at certain spatial scales and time periods relying on what was mentioned before, and meanwhile their effectiveness was relatively assessed. Accordingly, a case study was provided in Hengshui region of North China Plain, using multi-source temporal satellite imageries in multiple resolutions. The last results practically showed that the model and approach of remote sensing scale and scaling conversion were effective and available in the actual crop growth remote sensing monitoring, while preserving informational integrity of satellite imageries, and thus they are able to be more widely applied and further integrated into agricultural condition remote sensing monitoring systems.

2. MODELS AND METHODS

Though the term “scale” is widely used in different disciplines, it is inconsistently defined. Meentemeyer (1989) defined scale in relation to the absolute and relative representations of space in geo-sciences. Lam and Cao (1992, 1997) otherwise described four meanings of scale, namely, the cartographic, the geographical, the operational and the measurement scale. (1) The *cartographic or map scale* refers to the ratio of a distance on a map against the corresponding distance on the ground. A large-scale map covers a small area with a high detail, where a small-scale map covers a larger area with less detailed information. (2) The *geographical or*

observational scale, which refers to the size or spatial extent of the study, takes the opposite perspective. A geographic large-scale study covers a large area of interest as opposite to a geographic small-scale study covering a small area (Cohen et al., 2003). (3) The *operational scale*, called also *scale of action*, represents a level at which a certain process phenomenon is best observed. (4)The *measurement scale or resolution* means the resolution of the measurement scale, for instance a pixel size of the raster map (Dungan, 2001). In the context of remote sensing, scale is greatly concerned about the ability of a sensor system to record and display fine spatial detail as separated by its surroundings, and the instantaneous field of view (IFOV) of the sensor system which represents the ground area viewed by the sensor at a given instant in time (i.e., the former corresponding to spatial resolution and the latter to temporal resolution) and additionally, if a sensor onboard a satellite, the revisit cycle of the satellite (Su et al, 2001). Remote sensing imagery thus encapsulates two important aspects of scale, that is, grain and extent. Grain refers to the smallest distinguishable part of an object in an observation set (i.e. spatial resolution), while extent corresponds to the span of all detected entities (Allen and Hoeksstra, 1991) (i.e. the total area covered within an image swath). Therefore, a hierarchical scale model can be integratively developed in view of various remote sensing data in resolutions and presented into a multi-dimensional scale space, which is comprehensively associated with corresponding objects and features (e.g., attributes) in one’s own scale level (as is characterized with scale dependence, respectively) (See Figure 1).

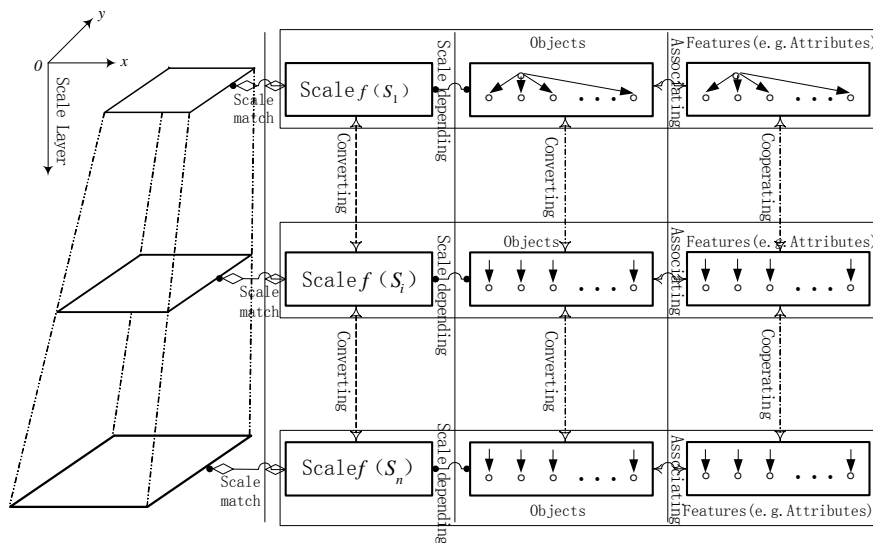


Figure 1. A multi-dimensional scaling space

Definition: Scale space transfer of remote sensing data: $F^i = F_1 \Theta F_2 \Theta \dots \Theta F_i : M_{all}^0(o, f(S_0)) \rightarrow M_{all}^i(o, f(S_i))$, where Θ is composite operator of resolution mapping functions, and $M_{all}^0(o, f(S_0))$ is the representation of available remote sensing data in the maximum resolution, and $M_{all}^i(o, f(S_i))$ is the representation of remote sensing data in the i -level resolution by reducing the surjective mapping.

2.1 Informational Associating Model, Based on Spatial Scaling of Satellite Images

According to different investigated aims, different associated information patterns are used to effectively and efficiently integrate and fuse varieties of multi-resolution remote sensing data. Multivariate (stepwise) regression analysis is an easy and available approach of associating information, such that we defined a general association model of remote sensing information in multi-resolution following below:

$$W(\omega_1, \omega_2, \dots, \omega_r) = \alpha_0 + \sum_{i=1}^n \alpha_i f_i(\omega_1(t_i), \omega_2(t_i), \dots, \omega_r(t_i); S_i) + \varepsilon \quad (1)$$

where α_0 is a constant; α_i is the i -th regression coefficient, $i = 1, 2, \dots, n$; $f_i(\omega_1(t_i), \omega_2(t_i), \dots, \omega_r(t_i); S_i)$ is a composite function of the varieties of remote sensing image information $\omega_1, \omega_2, \dots, \omega_r$ in the S_i -th spatial resolution during the t_i -th time period; ε is random noise factor.

2.2 Calculation of Similarity

Owing to the above formula (1), it is known whether varieties of remote sensing image information $\omega_1, \omega_2, \dots, \omega_r$ of some object area in multiple resolutions during corresponding time periods are able to be appropriately integrated and fused or not is very closely interrelated with their similarity. There are lots of methods of calculating similarity of remote sensing information, and then we select the common K -Nearest Neighbour (k -NN) method (Xu, 2002). A similarity of any matching pixels of remote sensing image data in some spatial resolution based in time series can thus be calculated by the following formula:

$$\begin{aligned} sim(\omega_j(t_i), \omega_j(t_{i+k})) &= \frac{\sum_{i=1}^{n-k} (\omega_j(t_i) - \bar{\omega}_j(t_i)) (\omega_j(t_{i+k}) - \bar{\omega}_j(t_{i+k}))}{\sqrt{\sum_{i=1}^{n-k} (\omega_j(t_i) - \bar{\omega}_j(t_i))^2 \cdot (\omega_j(t_{i+k}) - \bar{\omega}_j(t_{i+k}))^2}} \quad (2) \end{aligned}$$

where $\bar{\omega}_j(t_i) = \sum_{i=1}^{n-k} \mu_i \omega_j(t_i)$; $\bar{\omega}_j(t_{i+k}) = \sum_{i=1}^{n-k} \mu_i' \omega_j(t_{i+k})$, $j = 1, 2, \dots, k$; μ_i and μ_i' are weight factors, respectively.

2.3 Detection of Consistency

The consistency of local and overall spatial features of remote sensing images is usually represented by the relevance or similarity of image statistic, which can be measured in terms of matched conditions between objects or pixels of and associated attributes of the images (Wang et al, 2007; Li et al, 2005). Geary's C is a common measure of spatial autocorrelation, which is very available to assess the complex global or local correlation, spatial distribution pattern and significance level, etc., of adjacent observations in reference to spatial location (namely, bi-directional spatial variables in two-dimensional scale space) (Cliff and Ord, 1981; Ma et al, 2007). In the study, we helpful amended the kernel models of the Geary's C analysis method so as to meet the needs of application, as is shown below on the global and local statistic, i.e. C and C_i , respectively:

$$C = \frac{(n-1) \sum_{i=1}^n \sum_{j=1}^n w_{ij} (\omega_i^{(m)} - \bar{\omega}^{(m)})^2}{2 \left(\sum_{i=1}^n (\omega_i^{(m)} - \bar{\omega}^{(m)})^2 \right) \left(\sum_{i=1}^n \sum_{j=1, j \neq i}^n w_{ij} \right)} \quad (3)$$

$$C_i = \sum_{j \neq i}^n w_{ij} (z_i - z_j)^2 \quad (4)$$

where $\omega_i^{(m)}$ is the measurement of the m -th variety of remote sensing information in the i -th spatial unit (location); $\bar{\omega}^{(m)}$ is mean value of all variable $\omega_i^{(m)}$; $\{w_{ij}\}$ is spatial contiguity (weight) matrix with the alternative value that is entered with a 1 if two spatial objects are contiguous according some distance principle, or else entered with a 0; $[w_{ij} = (w_{ij}' p_{ij}) / \sum_{j=i}^n w_{ij}' p_{ij}]$ is a conditional spatial contiguity (weight) matrix with row normalization; p_j is a conditional probability ($P(X = x_j | X \neq x_i)$); z_i and z_j are two normalized variables, where $z_i = (\omega_i^{(m)} - \bar{\omega}^{(m)}) / \delta$ and δ is the standard deviation of all variable $\omega_i^{(m)}$.

Geary's c statistic C/C_i generally lies within the range of 0 to 2, with 1 being the expected value when there is no spatial autocorrelation that represents spatial random distribution pattern of investigated objects (or samples). That it is a value between 0 and 1 means positive spatial autocorrelation (i.e., being strongly positive at 0), which represents spatial aggregate distribution of the objects (or samples). Larger than 1 means negative spatial autocorrelation through to 2 that is strongly negative, which represents spatial dispersion distribution of the objects (or samples) (i.e., trending towards spatial aggregate distribution of the inverse objects). Hence, we statistically infer the global or local spatial consistency of varieties of corresponding remote sensing image data in accordance with the previous contents.

3. SITE DESCRIPTION AND DATA PREPARATION

3.1 Study Area

Huanghuaihai Plain, an alluvial-flood plain, lies in north China, and ranges from 113°E to 120°E and 32°N to 42°N, including Hebei, Henan, and Shandong provinces, and part of Beijing and Tianjin regions. The site covers 3.2×10^5 km² in the temperate zone with sub-humid continental monsoon climate, as well as characterised with the annual accumulated temperature (≥ 0 °C) of 4800 °C•d, annual average rainfall of 600mm per year, cumulative radiation doses of more than 5200MJ/m², and non-frost period of more than 200 days. It is one of China's important grain production bases, with the farming system of main food crops (i.e., winter wheat and summer maize for two-season crop in one year) (Ren et al, 2006). The study site, called Hengshui area, is located in centre of Huanghuaihai Plain and southeast of Hebei province, and cover 8815km² with the total population of about 4.07 million and jurisdiction over two county-level cities and four counties. It is a typical winter wheat cropping area under available natural conditions and higher than average national level of

China in per capita area of arable land. Hence, an in-depth study of the area is very significant for effective agricultural condition remote sensing monitoring in the HuangHuaiHai Plain, especially for winter wheat growth monitoring and regional yield estimation using remote sensing technology in the regions.

3.2 Data preparation

Due to the specific phenological characteristics in the site, we selected critical growth stages of winter wheat from March to May in 2005. The stages are featured with very active photosynthesis of, and significant to biological efficiency of PAR (photosynthetically active radiation) conversion to dry matter and final yield of winter wheat, and etc, such as the turning green, erecting, shooting stage, heading stage, filling, and milk stages (Ren et al, 2006).

The study, therefore, was performed using data derived from the sensors MODIS (Moderate-resolution Imaging Spectroradiometer, spatial resolutions of 250m & 500m) aboard EOS Aqua and Terra satellites, and AVHRR (Advanced Very High Resolution Radiometer, a spatial resolution of 1km) aboard NOAA-17 meteorological satellite, respectively. Such monthly time-series data, namely being from March to May in 2005, are available free of charge at the Web site of NASA (<http://ladsweb.nascom.nasa.gov/data/>).

The data were commonly processed by series of operations, mainly including calibrations (e.g., the sensor related corrections, earth-sun distance correction, solar zenith angle correction, and TOA (top-of-atmosphere) reflectance correction), cloud detection, radiometric correction, geometric correction, BRDF (bi-directional reflectance distribution function) correction, and NDVI (normalized difference

vegetation index) and LAI (leaf area index) compositing processes, etc. Then, the corresponding data products were obtained, and the time-series datasets of monthly NDVI and LAI fields, in instance, were further retrieved and gained from them, respectively.

In order to decrease effects of non-winter wheat growth areas, the ratios of winter wheat growth area versus total of sample frequencies in the associated counties (i.e., the values of winter wheat growth area divided through the total of remotely sensed image pixels of corresponding counties) were used to represent the differences of winter wheat growth areas in the study site, and the relative samples were discarded, the winter wheat growth areas of which were little to certain extent (namely, less than 10% in a pixel). The NDVI and LAI composite values were sequentially calculated with weighted average method in accordance with the foregoing ratios, respectively, and useful for winter wheat growth monitoring and yield estimation.

Additionally, the study used the winter wheat output data, based on the official statistic in 2005, to test corresponding accuracy of winter wheat output estimation and other involved data.

4. RESULTS AND DISCUSSION

4.1 Scale Effects of Spatial Consistency for NDVI and LAI data in the Study site

Using the related techniques and methods of spatial autocorrelation measure (Wang et al, 2007), spatial consistencies of NDVI and LAI data during different growing periods of winter wheat were obtained at multiple scales (resolutions) in the study site.

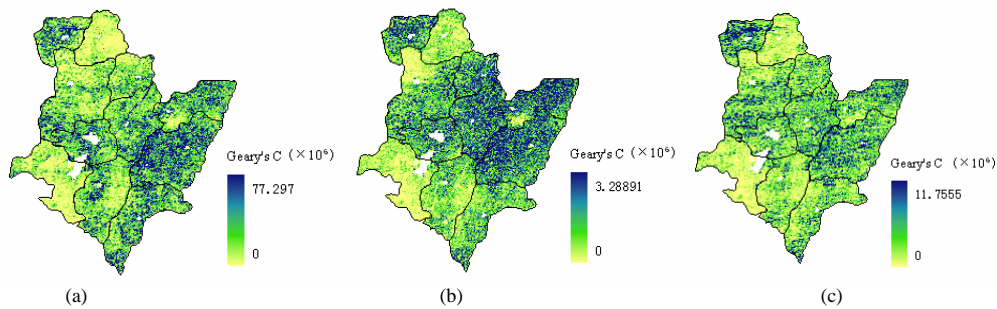


Figure 2. Spatial consistencies of vegetation indices of winter wheat growths during March period: (a)~(c) for NDVI in the resolutions of 250, 500m and 1km

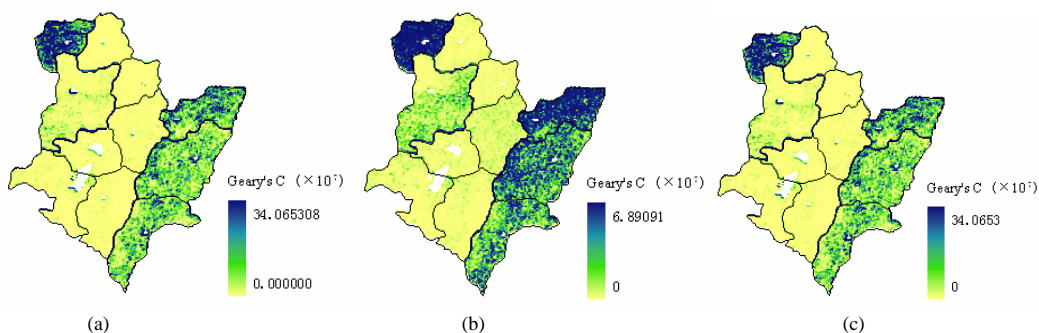


Figure 3. Spatial consistencies of vegetation indices of winter wheat growths during April period: (a)~(c) for NDVI in the resolutions of 250, 500m and 1km

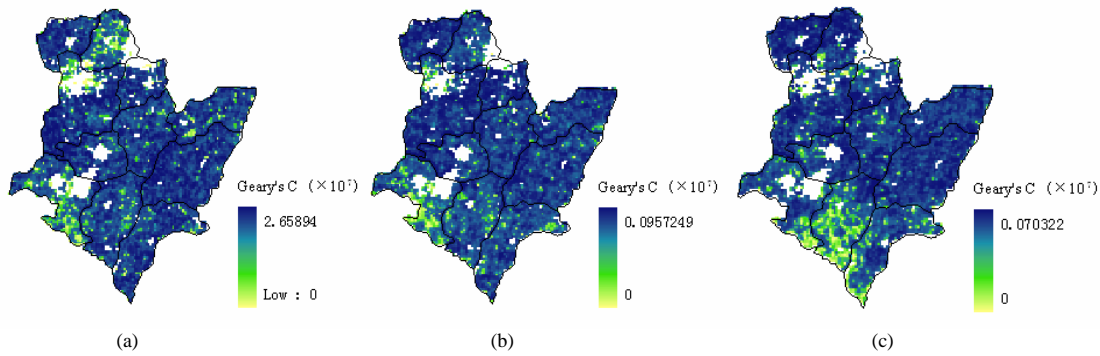


Figure 4. Spatial consistencies of vegetation indices of winter wheat growths during May period: (a)~(c) for NDVI in the resolutions of 250, 500m and 1km

Figure 2, 3 and 4 show that there were high consistencies of local spatial autocorrelation for retrieved NDVI and LAI data from MODIS and AVHRR image data in the resolutions of 250m, 500m and 1km, while being during winter wheat growing periods of March, April and May, respectively.

Meanwhile, consistencies of global spatial autocorrelation for retrieved NDVI and LAI data in multi-resolution were quite desirable during the time-series periods, as were shown in APPENDIX A: the Geary's C statistic of the NDVI and LAI data were 0.05651, 0.01835 and 0.04751 in 250m resolution; 0.08244, 0.02684 and 0.04751 in 500m resolution; and 0.02547, 0.02969 and 0.05605 in 1km resolution, respectively. The spatial distributions of winter wheat are thus greatly consistent, though there are largely different agronomic characters during different growing periods of the crop, so it is obvious that the law become a underlying statistical basis with respect to crops growth monitoring, especially in yield estimation of winter wheat, employing remote sensing technology.

4.2 Effectively Synthetic Pattern of Retrieved NDVI and LAI in Multi-resolution

According to the models and algorithms in Section 2.2 and of NDVI-LAI relationship (Huang et al, 1996; Meng, 2006), similarities of monthly retrieved NDVI and LAI data in the main growth periods (i.e., March to May) of winter wheat in the year (2005) were obtained based at different resolutions in the study site. As is followed below in Figure 5, the similarities in time series were very significant and further illustrated the spatial consistencies of winter wheat characters in different growth periods (see Section 4.1).

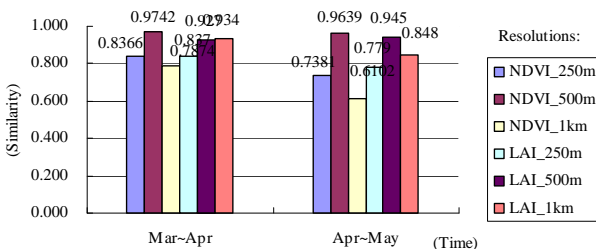


Figure 5. Relationship of time-series NDVI and LAI of winter wheat during mainly growing periods, respectively

To date, the multivariate (stepwise) regression analysis was performed to simulate the growth conditions of and yield

estimation of winter wheat in terms of the foregoing content mentioned in Section 2.1. In APPENDIX B and C, the solution of Mode_4 showed both its related coefficient (R^2) and Significance F were bigger, and it should thus be the most optimal and selected in practice. Therefore, it is greatly important how to select and utilize the models and methods for agricultural condition monitoring (esp. in crops yield estimation) based on multi-source remotely sensed data (in different spatial and temporal resolutions), for example, accuracy and validity of agricultural condition remote sensing monitoring are seriously affected, so it is a kernel bottleneck of agricultural condition remote sensing monitoring technology and needs to more deeply be explored and investigated in practical application.

5. CONCLUSION

Remotely sensed data at multiple scales are widely used to monitor agricultural conditions, and the synthetically applied approaches, based on varieties of data (including remotely sensed data), are thus available and successful to some extent in crop yield estimation. In the other hand, crop yield remote sensing estimation is very greatly complex and difficult because its feasibility and practicability, for example, are not only taken into account, but also do reliability and accuracy in practical application. Hence, it is necessary and significant to synthetically analyse characteristic parameters of crops growth and phenological law and discover scale effects of remotely sensing data, and then present scale and scaling models, that is, an effective and essential means to improve accuracy of crops yield estimation using remote sensing techniques.

In this study, the scale problem and scale effect of multi-source remotely sensed image data were present and investigated. The authors, thus, theoretically illuminated multi-scale space of remotely sensed data, and proposed the mapping models of scaling and assessed accuracies of the models. In practice, the synthetic model, based on remote sensed image and multiple vegetation-indices data at multi-scale, is more adoptable and more accurate in crops yield estimation than is a variety of remote sensed image and vegetation index.

At last, it should be pointed out that: so far, approaches of synthetically applying multi-source remotely sensed data at multi-scale are still developed at a primer level, for example, only primarily taking into account small difference effect of the vegetation indices parameters (i.e., NDVI and LAI) retrieved from multi-source remotely sensing data that were resulted in

by the spectral band placement of the satellite sensors, and then need to yet be improved; and methods and workflows of remotely sensed data preprocess are much trivially complicated, so they need to further be modified usefully; moreover, it is required, too, to develop new patterns, methods and models of accuracy check and assessment of crops yield estimation in order to enhance their validity. In addition, to fully understand potential mechanisms of corresponding specific remote sensing information is able to make it easy to utilize them in information scaling conversion across scales and to enhance accuracy of agricultural condition monitoring; and maybe, how to soundly integrate remotely sensed data with non-remotely-sensed data further proceeds further to be solved and developed in this direction.

REFERENCES

- Allen, T.F.H., and T.W. Hoekstra., 1991. Role of heterogeneity in scaling of ecological systems under analysis. *Ecological Studies*, 86, pp.47-68.
- Atkinson P. M. and Curran P. J., 1995. Defining an optimal size of support for remote sensing investigations. *IEEE Transactions on Geoscience and Remote Sensing*, 33 (3), pp.768-776.
- Bo Y. C., Wang J. F., 2003. Uncertainty in Remote Sensing, Classification and Scale Effect Modeling. *Geological Publishing House*, pp.68-93.
- Cao, C., Lam, N.S., 1997. Understanding the scale and resolution effects in remote sensing and GIS. In: *Quattrochi, D.A., Goodchild, M.F. (Eds.), Scale in Remote Sensing and GIS*. Boca Raton, FL, pp. 57-72
- Cliff A D, Ord J., 1981. *Spatial Models and Applications*. Pion, London.
- Cohen, W. B., Maier-sperger, T. K., Yang, Z., Turner, D. P., Ritts, W. D., Berterreche, M., Gower, S. T., Running, S. W., 2003. Comparisons of land cover and LAI estimates derived from ETM+ and MODIS for four sites in North America: a quality assessment of 2000/2001 provisional MODIS products. *Remote Sensing of Environment*, 88(3), 233-255.
- Dungan, J. L. 2001. Scaling up and scaling down: relevance of the support effect on remote sensing of vegetation. In *Modelling Scale in Geographical Information Science*, eds. N. J. Tate and P. M. Atkinson, Hoboken, NJ: John Wiley and Sons, pp. 221-236.
- Huang J. F., Xie G. H., 1996. *Synthetically meteorological satellite remote sensing models for winter wheat and application*. China Meteorological Press, pp.38-54.
- Lam N., and Quattrochi D. A., 1992. On the issues of scale, resolution, and fractal analysis in the mapping sciences. *The Professional Geographer*, 44, pp.88-98.
- Li L., Wu F., 2005. *The multi-scale Models of geo-spatial data and visualizing approaches*. Since press, pp. 80-84.
- Liu Y. C., Fan L. X., 2004. On Scale Issues of Remote Sensing in Forestry. *Journal of Northwest Forestry University*, 19(4), pp. 165-169.
- Ma R. H., Pu Y. X., Ma X. D., 2007. *Mining Spatial Association Patterns from GIS Database*. Since press, pp. 102-111.
- Markham B L and Townshend J. R. G., 1981. Landcover Classification Accuracy as a Function of Sensor Spatial Resolution. In: *15th International Symposium of Remote Sensing of environment*. Ann Arbor, MI, United States, pp. 1075-1090. 1981.
- Meentemeyer, V., 1989. Geographical perspectives of space, time, and scale, *Landscape Ecology*, 3(3/4), pp. 163-173.
- Meng J. H., 2006. *Research to Crop Growth Monitoring Indicators with Remote Sensing*. Ph. D. Dissertation. Institute of Remote Sensing and Application. Chinese Academy of Sciences.
- Mo L. L., Wu B. F., Yan N. N., Huang H. P., Li Q. Z., 2007. Validation of Agricultural Drought Indices and Their Uncertainty Analysis. *Bulletin of Soil and Water Conservation*, 27(2), pp.119-122.
- Qian Y. L., Yang B. J., Lei Y. W., 2004. Data fusion and its application prospect in agricultural condition monitoring using remote sensing. *Transactions of the Chinese Society of Agricultural Engineering*, 20(4), pp.286-290.
- Ren J. Q., Chen Z. x., Tang H. J., Shi R. X., 2006. Regional yield estimation for winter wheat based on net primary production model. *Transactions of the CSAE*, 22(5), pp.111-117.
- Su L. H., Li X. W., Huang Y. X., 2001. Department of Geography and Center for Remote Sensing. *Advance in Earth sciences*, 16(4), pp.544-548.
- Wang Y. F., He H. L., 2007. *Method of spatial data analysis*. Since press, pp. 95-119.
- Woodcock C. E. and Strahler A. H., 1987. The factor of scale in remote sensing. *Remote Sensing of Environment*, 21(3), pp.311-332.
- Wu B. F., Li Q. Z., 2004. Crop Acreage Estimation Using Two Individual Sampling Frameworks with Stratification. *Journal of Remote Sensing*, 8(6), pp.551-569.
- Xu J. H., 2002. *Mathematical Methods in Contemporary Geography*. High Education Press, pp.60-69.

ACKNOWLEDGEMENTS

This study is supported by the China National High Technology Research and Development Program (863 Program) Project (No. 2006AA12Z103), China National Key Technologies R&D Program Project (No. 2006BAD10A06), China Postdoctoral Science Foundation (No. 20070420440) and "Multisensor remote sensing cooperative retrieval and its application in agriculture monitoring automatization" (RDA0813). The authors thank EOS Gateway and LPDAAC for the MODIS data.

APPENDIX A. SPATIAL CONSISTENCIES OF NDVI OF WINTER WHEAT TIME-SERIES GROWTHS AT MULTIPLE SCALES IN STUDY AREAS*

Time Series	Resolution (Scale)	St.Dev. (Nor.)	St.Dev. (Rand.)	Z (Norm.)	Z (Rand.)	C
March	250m	0.00192	0.00192	492.14642	492.56123	0.05651
	500m	0.00385	0.00389	254.89363	252.44596	0.01835
	1k	0.00827	0.00819	115.21961	116.29202	0.04751
April	250m	0.00192	0.00191	478.62323	479.41602	0.08244
	500m	0.00385	0.00393	252.68765	247.6844	0.02684
	1k	0.00827	0.00819	115.21961	116.29202	0.04751
May	250m	0.00192	0.00191	508.34068	509.09622	0.02547
	500m	0.00385	0.00389	251.94761	249.47571	0.02969
	1k	0.00827	0.00823	114.18656	114.71944	0.05605

*To note: St.Dev. and Z are Standard Deviation and Significance at the Normalized or Randomized, respectively; C is geary's C.

APPENDIX B. COMPARISON OF SYNTHETIC REGRESSION MODELS OF NDVI AND LAI DATA IN DIFFERENT RESOLUTIONS BY CROSS-TEST

ID	Scale Space (Resolutions)	Regression Models (T)	R ²	Significance F
Mode_1	250m	$W^{(1)} = -114343.95 + 236.5128 * \overline{NDVI}_s^{(Mar,250m)} - 4.5865 * \overline{LAI}_s^{(Mar)} - 82.0939 * \overline{NDVI}_s^{(Apr)}$ $- 9.4960 * \overline{LAI}_s^{(Apr)} + 34.2301 * \overline{NDVI}_s^{(May)} + 4.2612 * \overline{LAI}_s^{(May)}$	0.73696	0.28390
Mode_2	500m	$W^{(1)} = 70434.6871 - 20.0951 * \overline{NDVI}_s^{(Mar)} + 7.5249 * \overline{LAI}_s^{(Mar)} + 213.5692 * \overline{NDVI}_s^{(Apr)}$ $+ 7.4142 * \overline{LAI}_s^{(Apr)} - 243.8725 * \overline{NDVI}_s^{(May)} - 2.5281 * \overline{LAI}_s^{(May)}$	0.80134	0.17875
Mode_3	1km	$W^{(1)} = 21353.6328 + 1223.9888 * \overline{NDVI}_s^{(Mar)} + 153.2817 * \overline{LAI}_s^{(Mar)} + 260.1135 * \overline{NDVI}_s^{(Apr)}$ $- 36.7849 * \overline{LAI}_s^{(Apr)} - 524.7642 * \overline{NDVI}_s^{(May)} + 50.8384 * \overline{LAI}_s^{(May)}$	0.70485	0.33976
Mode_4	Synthetic Scale Space (in 250m, 500 and 1km)	$W^{(1)} = -358217.1178 + 163.5827 * \overline{NDVI}_s^{(Mar,250m)} - 11.5456 * \overline{LAI}_s^{(Mar,250m)} + 25.6784 * \overline{NDVI}_s^{(Apr,500m)}$ $- 3.7322 * \overline{LAI}_s^{(Apr,500m)} + 1727.6933 * \overline{NDVI}_s^{(May,1km)} - 142.1289 * \overline{LAI}_s^{(May,1km)}$	0.70651	0.33684
To Note	The above models as to yield estimation of winter wheat; \overline{NDVI}_s and \overline{LAI}_s are the mean values of retrieved NDVI and LAI (by winter wheat area ratios) in corresponding counties, respectively.			

APPENDIX C. COMPARISON OF SYNTHETIC REGRESSION MODELS OF NDVI AND LAI DATA IN DIFFERENT RESOLUTIONS IN THE STUDY AREAS BY CROSS-TEST (IN 2005)

County name	Model_1			Model_2			Model_3			Model_4		
	WWYE (T)	SV (T)	RE (%)	WWYE (T)	SV (T)	RE (%)	WWYE (T)	SV (T)	RE (%)	WWYE (T)	SV (T)	RE (%)
Anping	111692	100470	11.17	96692.1	100470	-3.76	58970.4	100470	-41.31	96072	100470	-4.38
Fucheng	148821	127974	16.29	133474	127974	4.3	137466	127974	7.42	149592	127974	16.89
Gucheng	170244	173579	-1.92	203893	173579	17.46	178167	173579	2.64	173239	173579	-0.2
Jing County	214467	247622	-13.39	226880	247622	-8.38	211252	247622	-14.69	240818	247622	-2.75
Jizhou	78161.2	99837	-21.71	78026.3	99837	-21.85	133929	99837	34.15	91231.5	99837	-8.62
Raoyang	69110	79175	-12.71	70911.3	79175	-10.44	59431.4	79175	-24.94	86987	79175	9.87
Shenzhou	202183	237075	-14.72	220660	237075	-6.92	214651	237075	-9.46	187611	237075	20.86
Wuqiang	44076.3	76176	-42.14	97604.7	76176	28.13	66662.7	76176	-12.49	70128.9	76176	-7.94
Zaoqiang	172545	134650	28.14	82387.1	134650	-38.81	125395	134650	-6.87	124368	134650	-7.64
To Note	WWYE-Winter Wheat Yield Estimation; SV-Statistic Value; RE-Relative Error; MRE-Mean RE.											

